

# Existence of the critical point in finite density lattice QCD

Shinji Ejiri

*Physics Department, Brookhaven National Laboratory, Upton, New York 11973, USA*

(Received 24 June 2007; published 18 January 2008)

We propose a method to probe the nature of phase transitions in lattice QCD at finite temperature and density, which is based on the investigation of an effective potential as a function of the average plaquette. We analyze data obtained in a simulation of two-flavor QCD using p4-improved staggered quarks with bare quark mass  $m/T = 0.4$  and find that a first order phase transition line appears in the high density regime for  $\mu_q/T \gtrsim 2.5$ . We also discuss the difference between the phase structures of QCD with nonzero quark chemical potential and nonzero isospin chemical potential.

DOI: [10.1103/PhysRevD.77.014508](https://doi.org/10.1103/PhysRevD.77.014508)

PACS numbers: 11.15.Ha, 12.38.Gc, 12.38.Mh

## I. INTRODUCTION

In the last several years remarkable progress has been made in numerical studies of lattice QCD at finite temperature ( $T$ ) and quark chemical potential ( $\mu_q$ ). The transition line, separating hadron phase and quark-gluon plasma (QGP) phase, was investigated from  $\mu_q = 0$  to finite  $\mu_q$  [1–5], and the equation of state was also computed at low density [3,6–9]. Among others, the study of the endpoint of the first order phase transition line in the  $(T, \mu_q)$  plane is particularly important both from the experimental and theoretical point of view. This existence of such a critical point is suggested by phenomenological studies [10–12]. The appearance of the critical endpoint in the  $(T, \mu_q)$  plane is closely related to hadronic fluctuations in heavy ion collisions and may be experimentally examined by an event-by-event analysis of heavy ion collisions.

Although many trials have been made to prove the existence of the critical endpoint by first principle calculation in lattice QCD, no definite conclusion on this issue is obtained so far. The first trial to find the critical endpoint by numerical simulations was performed in Ref. [2] investigating the finite size scaling behavior of Lee-Yang zeros in the complex  $\beta = 6/g^2$  plane. The difficulty in the Lee-Yang zero method for finite density QCD is discussed in Ref. [13]. The radius of convergence in the framework of the Taylor expansion of the grand canonical potential can establish a lower bound on the location of the critical endpoint [6,7,14]. There are also studies in which the behavior of the critical endpoint as a function of the quark masses is examined by using the property that a critical endpoint exists at  $\mu_q = 0$  in the very small quark mass region for QCD with three flavors having degenerate quark masses [15–17]. Moreover, studies by simulations of phase-quenched finite density QCD have been performed in Refs. [18–20].

The purpose of this study is to clarify the existence of the endpoint of the first order phase transition line in the  $(T, \mu_q)$  plane. We propose a new method to investigate the nature of transition. In the study of finite density lattice

QCD, the reweighting method [21,22] plays an important role. However, the calculation of physical quantities becomes increasingly more difficult for large  $\mu_q$  due to the sign problem [23,24]. We also consider a way to avoid the sign problem.

We evaluate an effective potential as a function of the average plaquette and identify the type of transition from the shape of the potential. The partition function can be written as

$$Z(\beta, \mu_q) = \int R(P, \mu_q) w(P) e^{-S_g(P, \beta)} dP, \quad (1)$$

where  $P$  denotes the plaquette value,  $S_g(P, \beta)$  is the gauge action,  $w(P)$  is the state density at  $\mu_q = 0$  for each  $P$ , and  $R(P, \mu_q)$  is the modification factor for finite  $\mu_q$ .  $R(P, \mu_q)$  is obtained by calculating the quark determinant  $\det M$  and is assumed to be real and positive. We then define the effective potential as  $V(P, \beta, \mu_q) = -\ln(Rw e^{-S_g})$ . If there is a first order phase transition point, where two different states coexist, the potential must have two minima at two different values of  $P$ . However, the calculation of the quark determinant is quite expensive and is actually difficult except on small lattices. Moreover, the sign problem is serious when we calculate  $R(P, \mu_q)$  directly.

This study is based on the following two ideas to avoid these problems. One is that we perform a Taylor expansion of  $\ln \det M(\mu_q)$  in terms of  $\mu_q$  around  $\mu_q = 0$  and calculate the expansion coefficients, as proposed in Ref. [3]. The Taylor expansion coefficients are rather easy to calculate by using the stochastic noise method. Although we must cut off this expansion at an appropriate order in  $\mu_q$ , we can estimate the application range where the approximation is valid for each analysis. While the application range of the Taylor expansion of  $\ln Z$  should be limited by the critical point because  $\ln Z$  is singular at the critical point, there is no such limit for the application range in the expansion of  $\ln R(P, \mu_q)$  because the weight factor should always be well defined. This discussion is given in Sec. III B.

The second idea is that we consider the probability distribution function in terms of the complex phase of the quark determinant  $\theta$  when  $P$  and  $|\det M|$  are fixed. We

assume the distribution function is well approximated by a Gaussian function, and perform the integration over  $\theta$ . If we adopt this assumption, the sign problem in the calculation of  $\ln R(P, \mu_q)$  is completely solved. This assumption is reasonable for sufficiently large volume and is suggested by the simulation results given in this study. We discuss this method in Sec. III C.

General remarks on the phase transition in lattice QCD are given in Sec. II, and an effective potential as a function of the average plaquette is introduced. We discuss the reweighting method for the study of the QCD phase structure at nonzero temperature and density in Sec. III. We evaluate the effective potential using data obtained with two-flavors of p4-improved staggered quarks in Ref. [7]. We also discuss the phase structure of QCD with isospin chemical potential. Our conclusions are given in Sec. IV.

## II. PROBABILITY DISTRIBUTION FUNCTION AND PHASE TRANSITION

The grand canonical partition function of lattice QCD is given by

$$Z(\beta, \mu_q) = \int \mathcal{D}U (\det M)^{N_f} e^{-S_g}, \quad (2)$$

and the expectation value of an operator  $\mathcal{O}$  is calculated by

$$\langle \mathcal{O} \rangle = \frac{1}{Z} \int \mathcal{D}U \mathcal{O} (\det M)^{N_f} e^{-S_g}, \quad (3)$$

where  $M(\mu_q)$  is the quark matrix.  $N_f$  is the number of flavors. When one uses a staggered type quark action,  $N_f$  is replaced by  $N_f/4$ .  $S_g(\beta)$  is the gauge action, which is given by a linear combination of the Wilson loops  $W_{\mu\nu}^{I \times J}(x)$ , where  $I \times J$ ,  $\mu\nu$ , and  $x$  are the size, direction, and position of the Wilson loop, respectively.  $\beta$  is a simulation parameter related to the gauge coupling  $g$  being  $\beta = 6/g^2$ . The simplest gauge action is the standard plaquette action given by the following equation,

$$S_g = -\beta \sum_{x, \mu > \nu} W_{\mu\nu}^{1 \times 1}(x). \quad (4)$$

Because the  $1 \times 1$  Wilson loop is defined on an elementary square (plaquette),  $W_{\mu\nu}^{1 \times 1}$  is usually called plaquette or plaquette variable.

In a Monte Carlo simulation, we generate configurations of link variables  $\{U_\mu(x)\}$  with the probability in proportion to the weight factor  $(\det M)^{N_f} e^{-S_g}$  and the state density of  $\{U_\mu(x)\}$ . The expectation value is then estimated by taking an average of the operator  $\mathcal{O}[U_\mu]$  over the generated configurations  $\{U_\mu(x)\}$

$$\langle \mathcal{O} \rangle_{(\beta)} \approx \frac{1}{N_{\text{conf}}} \sum_{\{U_\mu(x)\}} \mathcal{O}[U_\mu]. \quad (5)$$

We introduce a probability distribution function of the plaquette,  $w(P)$ , which is defined by

$$w(P) = \int \mathcal{D}U \delta(P' - P) (\det M)^{N_f} e^{6\beta N_{\text{site}} P}, \quad (6)$$

where  $\delta(x)$  is the delta function. For later discussions, we define the average plaquette  $P$  as  $P \equiv -S_g/(6\beta N_{\text{site}})$ . This is the average of the plaquette over all elementary squares for the standard gauge action, Eq. (4).  $N_{\text{site}} = N_s^3 \times N_t$  is the number of sites. Using the distribution function, the expectation value can be rewritten as

$$\langle \mathcal{O}[P] \rangle_{(\beta)} = \frac{1}{Z} \int \mathcal{O}[P] w(P) dP, \quad Z = \int w(P) dP, \quad (7)$$

for an operator given by the plaquette  $\mathcal{O}[P]$ . In the calculation of Eq. (6), we actually use an approximate delta function such as a box type function,  $\delta(x) \approx \{1/\Delta (\text{for } \Delta/2 < x \leq \Delta/2), 0 (\text{otherwise})\}$ , or a Gaussian function,  $\delta(x) \approx 1/(\Delta\sqrt{\pi}) \exp[-(x/\Delta)^2]$ . For the case of the box type, we can estimate  $w(P)$  by counting the number of configurations for each value of  $P$  with the width of box  $\Delta$ . As  $\Delta$  decreases, the approximation becomes better but the statistical error becomes large because the number of configurations in each block becomes small. Hence, we must adjust the size of  $\Delta$  appropriately.

Next, we discuss the shape of the probability distribution function. In general, the number of states increases exponentially as the gauge fields become random. On the other hand, the random configurations are exponentially suppressed by the weight factor  $\exp(6\beta N_{\text{site}} P)$ , since the plaquette is one when the gauge field is  $U_\mu(x) = 1$  uniformly (free gas limit) and  $P$  decreases as the configuration becomes random. Therefore, the most probable  $P$  is determined by the balance of the number of states and the weight factor, and the value of the plaquette variable distributes around the most probable value for each point and each configuration.

We first consider the case that there is no spatial correlation between the plaquette variables at each point and the volume is sufficiently large. In this case, the shape of the probability distribution as a function of the plaquette averaged over the space must be a Gaussian function. The central limit theorem tells us that the probability distribution of the average of the random numbers which have the same probability distribution is always of Gaussian type when the set of random numbers is large enough. We can apply this theorem in this case. Hence,

$$w(P) = \sqrt{\frac{6N_{\text{site}}}{2\pi\chi_P}} \exp\left[-\frac{6N_{\text{site}}}{2\chi_P} (P - \langle P \rangle)^2\right], \quad (8)$$

where  $\langle P \rangle$  is the expectation value of  $P$  and  $\chi_P$  is the susceptibility,

$$\langle P \rangle = \int P w(P) dP,$$

$$\chi_P \equiv 6N_{\text{site}} \langle (P - \langle P \rangle)^2 \rangle = 6N_{\text{site}} \int (P - \langle P \rangle)^2 w(P) dP. \quad (9)$$

We expect that  $w(P)$  is of Gaussian type also for more general interacting cases when the correlation length is much shorter than the size of the system. If we divide the space into domains which are larger than the correlation length and average the plaquette variables in these domains, the averaged plaquettes can be independent for each domain. When the number of domains is large, the distribution function as a function of the plaquette averaged over space must be a Gaussian function.

However, we do expect that the probability distribution function is not of Gaussian type for the following two cases. One is, of course, the case that the correlation length is not small in comparison to the size of the system because the above-mentioned argument cannot be applied. The other case is that the most probable values of plaquette is not unique. For this case, the whole space is separated into domains having different states, and the plaquette variables in each domain distribute around one of the most probable values of plaquette. Although, on the surface separating these domains, the most probable plaquette value may not be realized, the effect from the wall becomes smaller as the volume increases, since the effect from the wall increases as a function of the area of the wall. Consequently, the existence of the domain wall does not affect the probability in the infinite volume limit. The probability distribution function should then be flat in the range between these most probable values of  $P$  because the spatial average of  $P$  depends on the size of these domains but the probability does not change in this range. However, in a finite volume, the effect from the domain wall cannot be neglected, hence the distribution function has two peaks when the number of most probable values for  $P$  is two. Clearly the two exceptions discussed here correspond to the case at a second order phase transition point and at a first order phase transition point, respectively.

Here, it is convenient to introduce the effective potential defined by

$$V(P) = -\ln w(P). \quad (10)$$

As discussed above, the distribution function is normally written as  $w(P) \sim \exp\{- (6N_{\text{site}}/2\chi_P)(P - \langle P \rangle)^2\}$ . When one considers a Taylor expansion of  $V(P)$  around the minimum  $\langle P \rangle$ , where the slope of the potential  $dV/dP$  is zero, the effective potential is dominated by the second order term in the region near the minimum, i.e. the potential is a quadratic function in the vicinity of  $\langle P \rangle$ , and the second derivative (curvature) of  $V(P)$  at  $\langle P \rangle$  is related to the plaquette susceptibility with

$$\frac{d^2 V}{dP^2} = \frac{6N_{\text{site}}}{\chi_P}. \quad (11)$$

A second order phase transition point is characterized by the slope and curvature of the effective potential. The slope  $dV/dP$  and curvature  $d^2V/dP^2$  become zero simultaneously at the critical point. As given in Eq. (9),  $\chi_P$  is an indicator of fluctuations and diverges at a second order phase transition point in the thermodynamic limit. When the susceptibility  $\chi_P$  becomes large in the vicinity of a second order phase transition point, the effect from the second order term of  $V(P)$  becomes small in comparison to the higher order terms, and then the distribution function deviates from a Gaussian function. On the other hand, in the case of a first order phase transition point, more than one peak exist in the distribution function. This means that there are points which give  $dV/dP = 0$  more than once, and the curvature of  $V(P)$  may be negative around the mean value of  $P$ .

At the end of this section, we should also discuss the relation between the plaquette distribution function and the fourth order Binder cumulant,

$$B_4 \equiv \frac{\langle (P - \langle P \rangle)^4 \rangle}{\langle (P - \langle P \rangle)^2 \rangle^2}, \quad (12)$$

which often is used to identify the nature of a phase transition [25]. The value of the Binder cumulant at a second order critical point depends on the universality class. In the case of a first order phase transition, assuming the plaquette distribution is a double peaked function, the Binder cumulant is estimated as

$$B_4 = \frac{\int (P - \langle P \rangle)^4 w(P) dP}{(\int (P - \langle P \rangle)^2 w(P) dP)^2} \approx \frac{\Delta^4}{(\Delta^2)^2} \approx 1, \quad (13)$$

where the distance between two peaks is  $2\Delta$  and is wider than the width of each peak. On the other hand, when the distribution function can be modeled by a Gaussian function for a crossover transition or at a normal point, the Binder cumulant is given by

$$B_4 \approx \frac{\sqrt{x/\pi} \int (P - \langle P \rangle)^4 e^{-x(P - \langle P \rangle)^2} dP}{(\sqrt{x/\pi} \int (P - \langle P \rangle)^2 e^{-x(P - \langle P \rangle)^2} dP)^2} = \left( \frac{\sqrt{x}}{\pi} \frac{d^2 \sqrt{\pi/x}}{dx^2} \right) / \left( -\sqrt{\frac{x}{\pi}} \frac{d\sqrt{\pi/x}}{dx} \right)^2 = 3. \quad (14)$$

In a region where a first order phase transition changes to a crossover, the Binder cumulant changes rapidly from one to three. We expect to find such a region for full QCD at high temperature and density.

In addition, the method of Lee-Yang zeros has been used to identify the nature of the phase transition. The relation between the plaquette distribution function and the scaling analysis of the Lee-Yang zero has been discussed in Ref. [13]. The scaling behavior of the Lee-Yang zero can be also explained by the plaquette distribution function.

Hence, the distribution function of the plaquette plays an important role in the investigation of the nature of a phase transition.

### III. LATTICE QCD AT FINITE DENSITY

The most difficult problem for lattice studies at finite baryon density is that the Boltzmann weight is complex when the chemical potential is nonzero. In this case, the Monte Carlo method is not applicable directly, since configurations cannot be generated with a complex probability. A popular approach to avoid this problem is the reweighting method. We perform simulations at  $\mu_q = 0$ , and incorporate the remaining part of the correct Boltzmann weight for finite  $\mu_q$  in the calculation of expectation values. Expectation values  $\langle \mathcal{O} \rangle$  at  $(\beta, \mu_q)$  are thus computed by a simulation at  $(\beta_0, 0)$  using the following identity:

$$\langle \mathcal{O} \rangle_{(\beta, \mu_q)} = \frac{\langle \mathcal{O} e^{N_f (\ln \det M(\mu_q) - \ln \det M(0))} e^{6(\beta - \beta_0) N_{\text{site}} P} \rangle_{(\beta_0, 0)}}{\langle e^{N_f (\ln \det M(\mu_q) - \ln \det M(0))} e^{6(\beta - \beta_0) N_{\text{site}} P} \rangle_{(\beta_0, 0)}}. \quad (15)$$

This is the basic formula of the reweighting method. However, because  $\ln \det M(\mu_q)$  is complex, the calculations of the numerator and denominator in Eq. (15) becomes in practice increasingly more difficult for larger  $\mu_q$ . We define the phase of the quark determinant  $\theta$  by the imaginary part of  $N_f \ln \det M(\mu_q)$ . If the typical value of  $\theta$  becomes larger than  $\pi/2$ , the real part of  $e^{i\theta}$  ( $= \cos\theta$ ) changes its sign frequently. Eventually both the numerator and denominator of Eq. (15) become smaller than their statistical errors and Eq. (15) can no longer be evaluated. We call it the ‘‘sign problem.’’ The sign problem becomes more serious when the volume is large and the quark mass is small [23,24].

#### A. Reweighting method for finite $\mu_q/T$

Let us discuss the reweighting method for finite  $\mu_q$  using the plaquette distribution function. Originally, the reweighting method was proposed using the distribution function (histogram) in Ref. [21], and applications to the finite density QCD in this style have been discussed in Refs. [20,26–28].

Here and hereafter, we restrict ourselves to discuss only the case when the quark matrix does not depend on  $\beta$  explicitly, e.g. the standard Wilson and staggered quark actions, the p4-improved staggered quark action, etc., for simplicity. The partition function can be rewritten as

$$Z(\beta, \mu_q) = \int R(P, \mu_q) w(P, \beta) dP, \quad (16)$$

where  $w(P, \beta)$  is defined in Eq. (6) at  $\mu_q = 0$  and  $R(P, \mu_q)$  is the reweighting factor for finite  $\mu_q$  defined by

$$R(P', \mu_q) \equiv \frac{\int \mathcal{D}U \delta(P' - P) (\det M(\mu_q))^{N_f}}{\int \mathcal{D}U \delta(P' - P) (\det M(0))^{N_f}}. \quad (17)$$

This  $R(P, \mu_q)$  is independent of  $\beta$ , and  $R(P, \mu_q)$  can be measured at any  $\beta$  using the following identity:

$$\begin{aligned} R(P', \mu_q) &= \frac{\int \mathcal{D}U \delta(P' - P) (\det M(\mu_q))^{N_f} e^{6\beta N_{\text{site}} P}}{\int \mathcal{D}U \delta(P' - P) (\det M(0))^{N_f} e^{6\beta N_{\text{site}} P}} \\ &= \frac{\langle \delta(P' - P) (\det M(\mu_q) / \det M(0))^{N_f} \rangle_{(\beta, \mu_q=0)}}{\langle \delta(P' - P) \rangle_{(\beta, \mu_q=0)}}, \end{aligned} \quad (18)$$

where  $\langle \cdot \cdot \cdot \rangle_{(\beta, \mu_q=0)}$  means the expectation value at  $\mu_q = 0$ . In this method, all simulations are performed at  $\mu_q = 0$  and the effect of finite  $\mu_q$  is introduced through the operator  $\det M(\mu_q) / \det M(0)$  measured on the configurations generated by the simulations at  $\mu_q = 0$ . The expectation value of  $\mathcal{O}[P]$  is given by

$$\langle \mathcal{O}[P] \rangle_{(\beta, \mu_q)} = \frac{\int \mathcal{O}[P] R(P, \mu_q) w(P, \beta) dP}{\int R(P, \mu_q) w(P, \beta) dP}. \quad (19)$$

Moreover, the weight factor for nonzero  $\mu_q$  is  $R(P, \mu_q) w(P, \beta)$ , and thus the effective potential is defined by

$$\begin{aligned} V(P, \beta, \mu_q) &\equiv -\ln[R(P, \mu_q) w(P, \beta)] \\ &= -\ln R(P, \mu_q) + V(P, \beta, 0). \end{aligned} \quad (20)$$

The shape of the effective potential can then also be investigated at nonzero  $\mu_q$  once  $R(P, \mu_q)$  is obtained.

However, there are two problems to calculate  $R(P, \mu_q)$ . The first problem is that the calculation of the quark determinant  $\det M(\mu_q)$  is very expensive. With present day computer resources, the exact calculation of  $\det M(\mu_q)$  is difficult except on small lattices. The second problem is the sign problem. Because  $\ln \det M(\mu_q)$  is complex, the calculations of the numerator of Eq. (18) becomes in practice increasingly more difficult for larger  $\mu_q$ . If the complex phase factor of the quark determinant  $\text{Re}[e^{i\theta}]$  changes its sign frequently, the expectation value of  $R(P, \mu_q)$  becomes smaller than its statistical error and the calculation of  $-\ln R(P, \mu_q)$  in the effective potential becomes impossible.

#### B. Taylor expansion in terms of $\mu_q/T$

To avoid the first problem, we perform a Taylor expansion in terms of  $\mu_q$  around  $\mu_q = 0$  and calculate the expansion coefficients, as proposed in Ref. [3]. We expand  $\ln \det M(\mu_q)$  in a Taylor series,

$$\ln \left[ \frac{\det M(\mu_q)}{\det M(0)} \right] = \sum_{n=1}^{\infty} \frac{1}{n!} \left[ \frac{\partial^n (\ln \det M)}{\partial (\mu_q/T)^n} \right] \left( \frac{\mu_q}{T} \right)^n. \quad (21)$$

The Taylor expansion coefficients are rather easy to calcu-

late by using the stochastic noise method. Although we must cut off this expansion at an appropriate order of  $\mu_q$ , this approximation is valid at low density and can be systematically improved by increasing the number of the terms.

Here, we discuss the effect of a truncation of the expansion. To estimate the range of  $\mu_q/T$  where the approximation is valid, an analysis of the radius of convergence is useful. The radius of convergence for pressure  $p(T, \mu_q)$  is studied in Ref. [6]. When one performs a Taylor expansion for  $p/T^4 = \ln Z/(VT^3)$ ,

$$\frac{p(T, \mu_q)}{T^4} - \frac{p(T, 0)}{T^4} = \sum_{i=1}^{\infty} c_i(T) \left(\frac{\mu_q}{T}\right)^i, \quad (22)$$

the radius of convergence can be defined by

$$\rho = \lim_{i \rightarrow \infty} \rho_i, \quad \rho_i = \sqrt{\left| \frac{c_i}{c_{i+2}} \right|} \quad (23)$$

for  $i = 2, 4, 6, \dots$ , where the odd terms are zero because the partition function is an even function of  $\mu_q$ . The Taylor expansion converges in the range of  $\mu_q/T < \rho$  when we consider all order of the expansion coefficients. This radius of convergence determines the lower bound of the critical point. This means conversely that the upper limit of the application range must be below the critical point if we estimate thermodynamic quantities using the Taylor expansion coefficients of the pressure or  $\ln Z$ .

However, this problem may be avoidable when we consider a Taylor expansion of the reweighting factor  $R(P, \mu_q)$  in Eq. (16), since the weight factor itself should not be singular even at the critical point. Therefore, we expect that the application range is not limited by the critical point and evaluations beyond the critical point is possible. The same discussion of the radius of convergence is possible for the reweighting factor  $\ln R(P, \mu_q)$ . We define the expansion coefficients by

$$\ln R(P, \mu_q) = \sum_{i=1}^{\infty} r_i(P) \left(\frac{\mu_q}{T}\right)^i, \quad (24)$$

where the odd terms should be zero again. The radius of convergence is

$$\rho_i^{(R)} = \sqrt{\left| \frac{r_i}{r_{i+2}} \right|}. \quad (25)$$

When we neglect terms higher than  $O(\mu_q^n)$  in the calculation of  $\ln \det M$ , Eq. (21), the application range can be estimated by  $\mu_q/T \lesssim \rho_n^{(R)}$ . Because this approximation does not affect calculations of  $r_i(P)$  for  $i \leq n$ , the truncation error is negligible when the contribution from higher order terms is smaller than that from the lower order terms. In the range where  $\mu_q/T < \rho_n^{(R)}$ , the  $(n+2)$ th order term  $|r_{n+2}(\mu_q/T)^{n+2}|$  is smaller than the  $n$ th order term

$|r_n(\mu_q/T)^n|$ . Hence, the truncation error must be small in this range.

Before discussing the radius of convergence for  $\ln R(P, \mu_q)$  using the data obtained by Monte Carlo simulations, we estimate the application range at large  $P$  and small  $P$ , corresponding to large temperature and small temperature, respectively. In the free quark gas limit, where  $P$  is maximum, the quark determinant is expected to be  $(\ln \det M)(N_f/N_s)^3 = (7\pi^2/60) + (1/2) \times (\mu_q/T)^2 + (1/4\pi^2)(\mu_q/T)^4$  in the continuum limit [6]. Because  $\rho_4$  is infinity, the convergence of the Taylor expansion seems to be good for large  $P$ .

On the other hand, in the study of the equation of state [7,29], the numerical results of the derivatives of pressure with respect to  $\mu_q/T$  at low temperature have been found to reproduce the prediction from the hadron resonance gas model very well. Because small plaquette values are generated in the low temperature simulation, this model may give a suggestion of the application range for small  $P$ . The quark chemical potential dependence of pressure in the hadron resonance gas model is discussed in Ref. [29]. It is suggested that

$$\frac{p(\mu_q)}{T^4} - \frac{p(0)}{T^4} \propto \cosh\left(\frac{3\mu_q}{T}\right), \quad (26)$$

and the radius of convergence for pressure is given by

$$\rho_i = \sqrt{\frac{(i+2)(i+1)}{9}}. \quad (27)$$

This  $\rho_i$  increases as  $i$  increases, and the convergence radius  $\rho$  is infinity. Although we expect that the radius of convergence for  $\ln R$  is larger than that for the pressure, we try to estimate the application range from this  $\rho_i$ . When we neglect terms higher than  $O(\mu_q^6)$ , as it is done in this study, the application range is suggested to be  $\mu_q/T \lesssim \rho_6 \approx 2.5$ . This implies that the error that arises from the approximation up to  $O(\mu_q^6)$  may be sizeable for  $\mu_q/T \sim 2.5$ , and more careful arguments are required when we calculate the reweighting factor  $R(P, \mu_q)$  for  $\mu_q/T \gtrsim 2.5$ . We will discuss this application range in Sec. III F again. The results of  $\ln R(P, \mu_q)$  obtained by the calculations up to  $O(\mu_q^4)$  and  $O(\mu_q^6)$  will be compared, and we will confirm that the truncation error is still small even at  $\mu_q/T \sim 2.5$ .

### C. Avoidance of the sign problem at finite density

We discuss here how to avoid the sign problem in our reweighting approach. In the framework of the Taylor expansion, we can easily separate  $\ln \det M(\mu_q)$  into real and imaginary parts because the even derivatives of  $\ln \det M(\mu_q)$  are real and the odd derivatives are purely imaginary [3]. The absolute values of the quark determinant and the complex phases  $\theta$  are thus given by

$$\begin{aligned}
N_f \ln|\det M| &= N_f \operatorname{Re}[\ln(\det M)] \\
&= N_f \sum_{n=0}^{\infty} \frac{1}{(2n)!} \operatorname{Re} \frac{\partial^{2n}(\ln \det M)}{\partial(\mu_q/T)^{2n}} \left(\frac{\mu_q}{T}\right)^{2n},
\end{aligned} \tag{28}$$

$$\begin{aligned}
\theta &= N_f \operatorname{Im}[\ln(\det M)] \\
&= N_f \sum_{n=0}^{\infty} \frac{1}{(2n+1)!} \operatorname{Im} \frac{\partial^{2n+1}(\ln \det M)}{\partial(\mu_q/T)^{2n+1}} \left(\frac{\mu_q}{T}\right)^{2n+1},
\end{aligned} \tag{29}$$

where one must replace  $N_f$  in these equations to  $N_f/4$  when one uses a staggered type quark action. Here, it is worth noting that  $\theta$  corresponds to the complex phase of the quark determinant; however, by definition this quantity is not restricted to the range from  $-\pi$  to  $\pi$  because there is no reason that the imaginary part of  $\ln \det M$  in Eq. (29) must be in the finite range. In fact, this quantity becomes larger as the volume increases.

We show histograms of  $\theta$  at the pseudocritical temperature ( $\beta = 3.65$ ) for  $\mu_q/T = 1.0$  and  $2.0$  in Fig. 1, where  $\theta$  is calculated using the data of the Taylor expansion coefficients up to  $O(\mu_q^5)$  obtained with two flavors of p4-improved staggered quarks in Ref. [7]. These histograms seem to be almost Gaussian functions. We fit these data by Gaussian functions,  $\sim \exp(-x\theta^2)$ , where the overall factor and  $x$  are the fit parameters. The dashed lines in Fig. 1 are the fit results. It is found that the histogram of  $\theta$  is well represented by a Gaussian function.

Similar to the discussion of the Gaussian distribution function for the plaquette in Sec. II, we may argue that the histogram of  $\theta$  is a Gaussian function. Because there is no critical point in two-flavor QCD with finite quark mass at

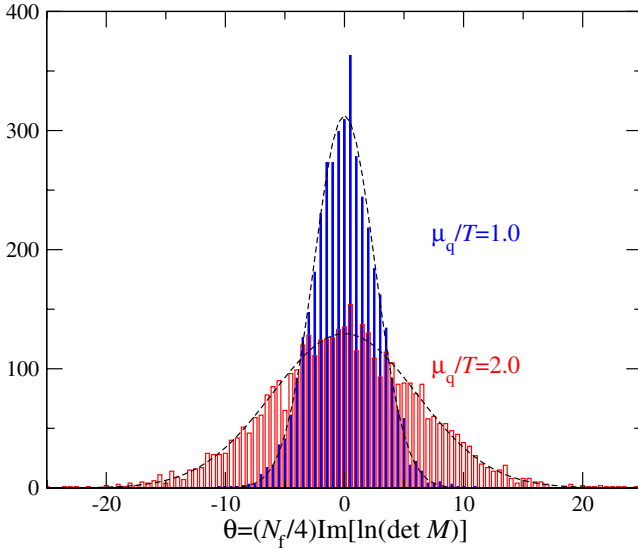


FIG. 1 (color online). The histogram of the complex phase for  $\mu_q/T = 1.0$  and  $2.0$  at  $\beta = 3.65$  ( $T/T_c = 1.00$ ) on a  $16^3 \times 4$  lattice. The dashed lines are the fit results by Gaussian functions.

$\mu_q = 0$ , the spatial correlation length between the quark fields is not expected to be long. The Taylor expansion coefficients in Eq. (29) are given by combinations of traces of products of  $\partial^n M / \partial(\mu_q/T)^n$  and  $M^{-1}$  (see appendix of Ref. [7]). Therefore, the expansion coefficients are obtained by the sum of the diagonal elements of such matrices. When the correlation among the diagonal elements is small and the volume is sufficiently large, the distribution functions of the expansion coefficients and  $\theta$  should be of Gaussian type due to the central limit theorem. For example, the diagonal elements of the first coefficient,  $\operatorname{Im}[\partial(\ln \det M) / \partial(\mu_q/T)] = \operatorname{Im}[\operatorname{tr}[M^{-1}(\partial M / \partial(\mu_q/T))]]$ , is the imaginary part of the local number density operator at  $\mu_q = 0$ . If the spatial density correlation is not very strong, the Gaussian distribution is expected. Figure 1 is consistent with this argument.

We note that, once we assume a Gaussian distribution for  $\theta$ , the problem of complex weights can be avoided. A variety of distribution functions with respect to various quantities are discussed in the density of state method [20,21,26–28]. We introduce the probability distribution  $\bar{w}$  as a function of the plaquette  $P$ , the absolute value of  $[\det M(\mu_q) / \det M(0)]^{N_f} \equiv F$ , and the complex phase  $\theta \equiv \operatorname{Im}[\ln F(\mu_q)]$ ,

$$\begin{aligned}
\bar{w}(P', |F|', \theta') &\equiv \int \mathcal{D}U \delta(P' - P) \delta(|F|' - |F|) \\
&\times \delta(\theta' - \theta) (\det M(0))^{N_f} e^{6\beta N_{\text{site}} P}.
\end{aligned} \tag{30}$$

The distribution function itself is defined as an expectation value at  $\mu_q = 0$ , i.e.  $\bar{w}(P', |F|', \theta') \propto \langle \delta(P' - P) \delta(|F|' - |F|) \delta(\theta' - \theta) \rangle_{(T, \mu_q=0)}$ ; however  $|F|$  and  $\theta$  are functions of  $\mu_q/T$  obtained by the Taylor expansion at  $\mu_q = 0$ . The expectation value of  $\mathcal{O}[P, |F|, \theta]$  at  $\mu_q = 0$  is given by

$$\begin{aligned}
\langle \mathcal{O}[P, |F|, \theta] \rangle_{(T, \mu_q=0)} &= \frac{1}{Z(\mu_q=0)} \int dP \int d|F| \\
&\times \int d\theta \mathcal{O}[P, |F|, \theta] \bar{w}(P, |F|, \theta).
\end{aligned} \tag{31}$$

Since the partition function is real even at nonzero density, the distribution function has the symmetry under the change from  $\theta$  to  $-\theta$ . Therefore, the distribution function is a function of  $\theta^2$ , e.g.,  $\bar{w}(\theta) \sim \exp[-(a_2\theta^2 + a_4\theta^4 + a_6\theta^6 + \dots)]$ . Moreover, as we discussed, when the system size is sufficiently large in comparison to the correlation length, the distribution function should be well approximated by a Gaussian function:

$$\bar{w}(P, |F|, \theta) \approx \sqrt{\frac{a_2(P, |F|)}{\pi}} \bar{w}'(P, |F|) \exp[-a_2(P, |F|)\theta^2]. \tag{32}$$

We assume this distribution function in terms of  $\theta$  when  $P$  and  $|F|$  are fixed.

The coefficient  $a_2(P, |F|)$  is given by

$$\begin{aligned} \frac{1}{2a_2(P', |F'|)} &= \int d\theta \theta^2 \bar{w}(P', |F'|, \theta) / \int d\theta \bar{w}(P', |F'|, \theta) \\ &= \frac{\langle \theta^2 \delta(P' - P) \delta(|F'| - |F|) \rangle_{(T, \mu_q=0)}}{\langle \delta(P' - P) \delta(|F'| - |F|) \rangle_{(T, \mu_q=0)}}, \end{aligned} \quad (33)$$

using  $\int \sqrt{a_2/\pi} \int \theta^2 \exp(-a_2\theta^2) d\theta = 1/(2a_2)$ .

$$\begin{aligned} \langle F(\mu_q) \delta(P' - P) \rangle_{(T, \mu_q=0)} &\approx \frac{1}{Z} \int dP \int d|F| \int d\theta \sqrt{\frac{a_2}{\pi}} \bar{w}'(P, |F|) e^{-a_2\theta^2} e^{i\theta} |F| \delta(P' - P) \\ &= \frac{1}{Z} \int dP \int d|F| \bar{w}'(P, |F|) e^{-1/(4a_2)} |F| \delta(P' - P) \\ &= \frac{1}{Z} \int \mathcal{D}U e^{-1/(4a_2(P, |F|))} |F(\mu_q)| \delta(P' - P) (\det M(0))^{N_f} e^{-S_g} \\ &= \langle e^{-1/(4a_2(P, |F|))} |F(\mu_q)| \delta(P' - P) \rangle_{(T, \mu_q=0)}. \end{aligned} \quad (34)$$

Since  $\theta$  is roughly proportional to the size of the quark matrix  $M$ , the value of  $1/a_2$  becomes larger as the volume increases. Therefore, the phase factor in  $R(P, \mu_q)$  decreases exponentially as a function of the volume. However, the most important point in this approach is that the operator in Eq. (34) is always real and positive for each configuration in this framework, hence the expectation value of  $R(P, \mu_q)$  is always larger than its statistical error, i.e. the contribution  $\ln R(P, \mu_q)$  to the effective potential  $V(P, \beta, \mu_q)$  is always well defined. Therefore, the sign problem is completely avoided if we can assume the Gaussian distribution of  $\theta$ .

We calculate  $\theta$  using the stochastic noise method. Then, the value of  $\theta$  contains an error due to the finite number of noise vectors ( $N_n$ ). As discussed in Ref. [3,24], a careful treatment is required to reduce this error for the calculation of  $\sqrt{\langle \theta^2 \rangle}$ , i.e. width of the distribution of  $\theta$ . Since the noise sets for the calculation of the two  $\theta$  in the product must be independent, we subtract the contributions from using the same noise vector for each factor. By using this method, we can make the  $N_n$  dependence of  $\sqrt{\langle \theta^2 \rangle}$  much smaller than that by the naive calculation from rather small  $N_n$ , hence it may be closer to the  $N_n = \infty$  limit. We took  $N_n = 50$  or 100 in this calculation, so that the  $N_n$  dependence is negligible. On the other hand, as  $N_n$  increases, the result of  $\sqrt{\langle \theta^2 \rangle}$  obtained by the naive calculation without the subtraction becomes smaller and approaches the result with the subtraction. For the case at  $\beta = 3.65$ ,  $\mu_q/T = 2.0$  with  $N_n = 100$  in Fig. 1, the difference between them is about 13%. Since the width of the distribution function shown in Fig. 1 corresponds to  $\sqrt{\langle \theta^2 \rangle}$  without the subtraction,

When the volume is sufficiently large, this assumption will be valid except at a critical point. For the case of two-flavor QCD at finite quark mass, this assumption should be valid because there is no critical point for  $\mu_q = 0$  except in the chiral limit, and is suggested by Fig. 1, though the values of  $P$  and  $|F|$  are not fixed in the calculation of Fig. 1. Then, the integration over  $\theta$  can be carried out easily and we obtain the numerator of Eq. (18) for the calculation of  $R(P, \mu_q)$ ,

tion, the width in Fig. 1 is slightly larger than that in the  $N_n = \infty$  limit.

For more quantitative arguments of the Gaussian distribution function, we also compute the fourth order Binder cumulant of the complex phase for  $\mu_q/T = 1.0$  and 2.0, using the data obtained in a simulation of two-flavor QCD with p4-improved staggered quarks, Ref. [7]. The Binder cumulant is defined by

$$B_4^\theta \equiv \frac{\langle \theta^4 \rangle}{\langle \theta^2 \rangle^2}. \quad (35)$$

As discussed in Sec. II, this quantity is a good indicator to check whether the distribution is of Gaussian or not. To confirm the validity of the assumption, Eq. (32), we should compute  $B_4^\theta$  as a function of  $P$  and  $|F|$ . However, because the width of the plaquette distribution function  $w(P, \beta)$  for each  $\beta$  is narrow in our simulation (see the results in Sec. III D), we calculate  $B_4^\theta$  for each  $\beta$  without separating the configurations in terms of  $P$ . The circle and square symbols in Fig. 2 are the results for  $\mu_q/T = 1.0$  and 2.0, respectively. We use the stochastic noise method for the calculation of the products of  $\theta$ . The results plotted by filled symbols are obtained when the contributions from using the same noise vector are subtracted. The open symbols are the results without the subtraction. Because the complex phase vanishes in the large  $\beta$  limit,  $\langle \theta^2 \rangle$  becomes smaller as  $\beta$  increases. We omitted results having large statistical errors due to the small  $\langle \theta^2 \rangle$  at large  $\beta$ . We find from this figure that the results of  $B_4^\theta$  are almost consistent with three. As we discussed in Sec. II, if the distribution is of Gaussian, the Binder cumulant is three. Hence, this figure suggests the Gaussian distribution. The

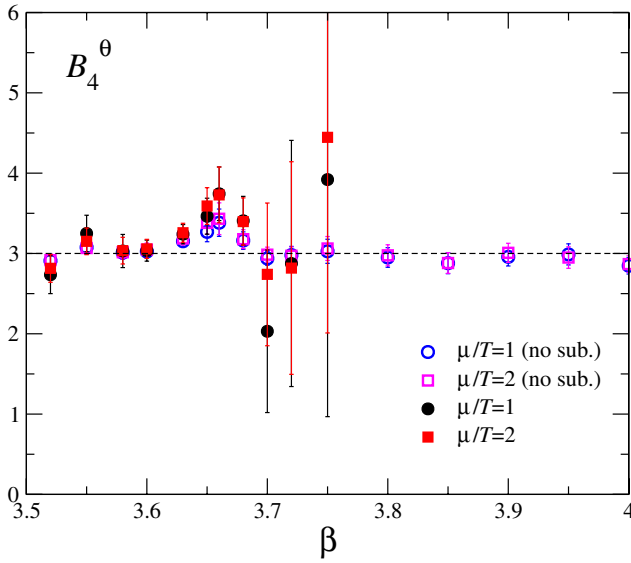


FIG. 2 (color online). The fourth order Binder cumulant of the complex phase for  $\mu_q/T = 1.0$  (circle) and 2.0 (square). The filled symbols are the results obtained when the contributions from using the same noise vector are subtracted in the products of  $\theta$ . The open symbols are the results without the subtraction. The dashed line is the value of Gaussian distribution.

results around  $\beta = 3.66$  are slightly larger than 3, but the difference would be within the systematic error due to finite statistics because usually the Binder cumulant becomes smaller than 3 when the correlation length is long.

To estimate the effect when the distribution is slightly different from Gaussian, we consider a distribution function with small  $a_4$ , i.e.  $\bar{w}(\theta) \sim \exp[-a_2\theta^2 - a_4\theta^4]$ . In this case, the phase factor changes from  $\exp[-1/(4a_2)]$  to  $\exp[-1/(4a_2) + 3a_4/(4a_2^3) - a_4/(16a_2^4) + \dots]$ , and also the expectation value of  $\theta^2$  for fixed  $P$  and  $|F|$  becomes  $\langle\theta^2\rangle = 1/(2a_2) - 3a_4/(2a_2^3) + \dots$ . Since the term of  $3a_4/(4a_2^3)$  is absorbed into  $\langle\theta^2\rangle/2$ , the leading contribution from  $a_4$  in the phase factor is  $\exp[-a_4/(16a_2^4)]$ . Because  $1/a_2 \sim O(\mu_q^2)$ , this effect becomes larger as  $\mu_q$  increases. Therefore, for the case of  $a_4 \neq 0$  ( $B_4^\theta \neq 3$ ), the estimation of the range of  $\mu_q$  in which the non-Gaussian contribution is small may be important as well as the application range of the Taylor expansion in  $\mu_q$  discussed in the previous section.

#### D. Reweighting method for $\beta$ direction

We consider the reweighting method for the  $\beta$  direction at  $\mu_q = 0$ . This is the case of  $R(P, 0) = 1$ . Using the plaquette distribution function (plaquette histogram)  $w(P, \beta_0)$  at the simulation point  $\beta_0$ , the expectation value of an operator given by the plaquette is evaluated by

$$\langle\mathcal{O}[P]\rangle(\beta) = \frac{\int \mathcal{O}[P] e^{6(\beta-\beta_0)N_{\text{site}}P} w(P, \beta_0) dP}{\int e^{6(\beta-\beta_0)N_{\text{site}}P} w(P, \beta_0) dP}, \quad (36)$$

where we discuss only the case when the quark matrix does not depend on  $\beta$  explicitly for simplicity, otherwise Eq. (36) is no longer correct.

From Eq. (36), under the parameter change from  $\beta_0$  to  $\beta$ , the weight  $w(P, \beta)$  becomes

$$w(P, \beta) = e^{6(\beta-\beta_0)N_{\text{site}}P} w(P, \beta_0). \quad (37)$$

If we rewrite  $e^{-6\beta_0 N_{\text{site}}P} w(P, \beta_0) \equiv w(P)$ , we obtain Eq. (1) from Eq. (16). The effective potential becomes

$$V(P, \beta) = -\ln w(P, \beta) = V(P, \beta_0) - 6(\beta - \beta_0)N_{\text{site}}P. \quad (38)$$

When  $\beta$  is increased, the slope of  $V(P)$  becomes smaller, whereas the curvature of  $V(P)$  does not change. This implies that the curvature of  $V(P)$  is independent of  $\beta$ . For the case of  $d^2V/dP^2 > 0$ , the value of  $P$  which gives the minimum of  $V(P)$  becomes larger as  $\beta$  increases.

Here, we want to explain the  $\beta$  dependence of the effective potential using the data from Ref. [7]. The configurations were generated with Symanzik-improved gauge and two-flavor p4-improved staggered fermion actions. Because the improved gauge action was used in Ref. [7], the definition of  $P$  is

$$P = -\frac{S_g}{6N_{\text{site}}\beta} = \frac{1}{6N_{\text{site}}} \left\{ \frac{5}{3} \sum_{x, \mu > \nu} W_{\mu\nu}^{1 \times 1}(x) - \frac{1}{12} \sum_{x, \mu \neq \nu} W_{\mu\nu}^{1 \times 2}(x) \right\}, \quad (39)$$

where  $W_{\mu\nu}^{I \times J}$  is the  $I \times J$  Wilson loop for each point and each direction. The maximum of this  $P$  is 1.5.

The probability distribution function  $w(P)$ , i.e. the histogram of  $P$ , and the effective potential  $V(P)$  are given in Fig. 3. These are measured at 16 simulation points from  $\beta = 3.52$  to 4.00 for the bare quark mass  $ma = 0.1$ . The corresponding temperature normalized by the pseudocritical temperature is in the range of  $T/T_c = 0.76$  to 1.98, and the pseudocritical point ( $T/T_c = 1$ ) is about  $\beta = 3.65$ . We show the values of  $\beta$  and  $T/T_c$  above these figures. The ratio of pseudoscalar and vector meson masses is  $m_{\text{PS}}/m_{\text{V}} \approx 0.7$  at  $\beta = 3.65$ . The lattice size  $N_{\text{site}}$  is  $16^3 \times 4$ . The number of configurations is 1000–4000 for each  $\beta$ . Further details on the simulation parameters are given in Ref. [7]. To obtain  $w(P)$  and  $V(P)$ , we grouped the configurations by the value of  $P$  into blocks and counted the number of configurations in these blocks, and the potential  $V(P)$  is normalized by the minimum value for each temperature.

Because the transition from the hadron phase to the quark-gluon plasma phase is a crossover transition for two-flavor QCD with finite quark mass, the distribution function is always of Gaussian type, i.e. the effective potential is always a quadratic function. The value of the plaquette at the potential minimum increases as  $\beta$  increases in accordance with the above argument.

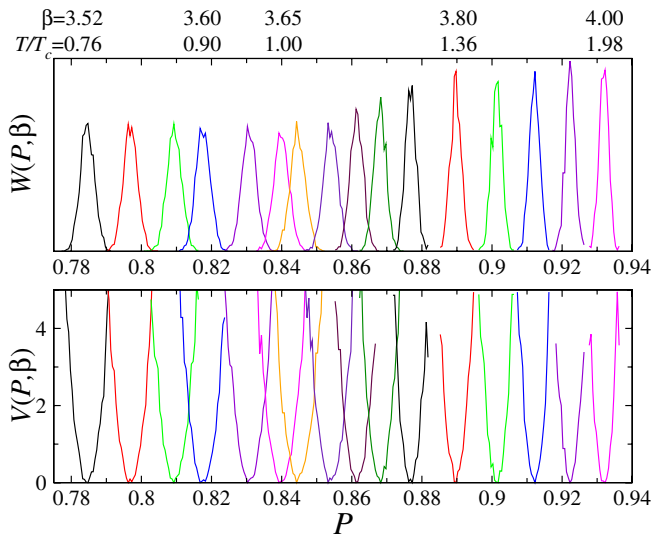


FIG. 3 (color online). The plaquette histogram and the effective potential at  $\mu_q = 0$  as a function of the plaquette for the two-flavor p4-improved staggered action obtained in Ref. [7].

Figure 4 shows the curvature of the effective potential at  $\mu_q = 0$ ,  $d^2V/dP^2(P) = -d^2(\ln w)/dP^2$ , as a function of  $P$ . We estimate this quantity from the relation between the plaquette susceptibility  $\chi_P$  and the curvature of the potential at  $\mu_q = 0$ , Eq. (11). Here, it should be emphasized again that the slope of the potential changes as Eq. (38) when  $\beta$  is changed, but the curvature of the potential never changes. This means that the curvature is independent of  $\beta$  and is determined by the measure  $\mathcal{D}U$  and the quark determinant  $\det M$ . As we discussed in Sec. II, the curvature of the effective potential  $V(P)$  at  $P$  for the potential minimum is important to categorize the nature of phase transition, e.g. the curvature must be zero at a second order phase transition. The property of the curvature being

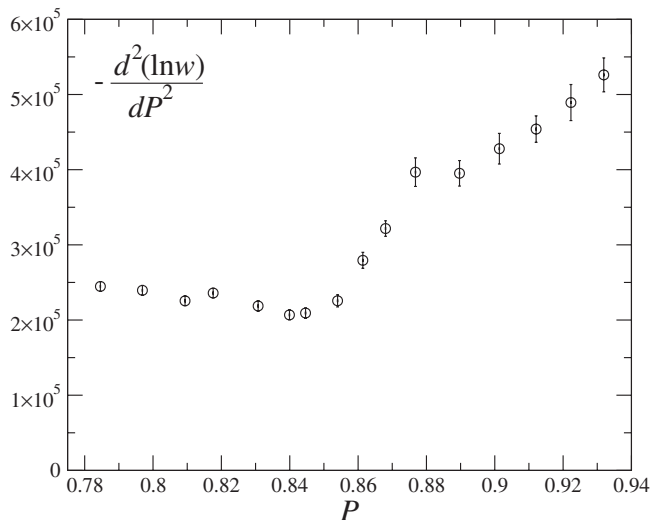


FIG. 4. The curvature of the effective potential at  $\mu_q = 0$ .

independent of  $\beta$  will make our analysis simpler in the next section.

### E. Numerical calculations of the reweighting factor

We calculate the probability distribution function at nonzero  $\mu_q$  using the data of the Taylor expansion coefficients up to  $O(\mu_q^6)$  computed in Ref. [7] with the p4-improved staggered quark action. Since the simulations are performed in the region where no critical points exist, the assumption of the Gaussian function is valid. The coefficient  $a_2(P, |F|)$  in the distribution function of  $\theta$  is measured using Eq. (33). However, because the values  $P$  and  $|F| = |\det M(\mu_q)/\det M(0)|^{N_f}$  on each configuration are strongly correlated [24], we may assume that  $|F|$  is approximately given as a function of  $P$  for each configuration so that  $a_2(P, |F|)$  is given by a function of  $P$  only. In this approximation, the contribution from the complex phase in  $R(P', \mu_q)$  can be simplified,

$$R(P', \mu_q) \approx e^{-1/(4a_2(P'))} \frac{\langle |F(\mu_q)| \delta(P' - P) \rangle_{(T, \mu_q=0)}}{\langle \delta(P' - P) \rangle_{(T, \mu_q=0)}}. \quad (40)$$

Although the correlation between  $|F|$  and  $a_2$  is neglected in this equation, the main contribution to the variation of  $R(P, \mu_q)$  comes from  $|F|$ , and the contribution from the phase factor is not very large, as we will see in Fig. 5. Therefore, the correlation of these two factors is negligible in the following argument. For the calculation of  $R(P, \mu_q)$ , we use the delta function approximated by a Gaussian function,  $\delta(x) \approx 1/(\Delta\sqrt{\pi}) \exp[-(x/\Delta)^2]$ , where  $\Delta = 0.0025$  is adopted.

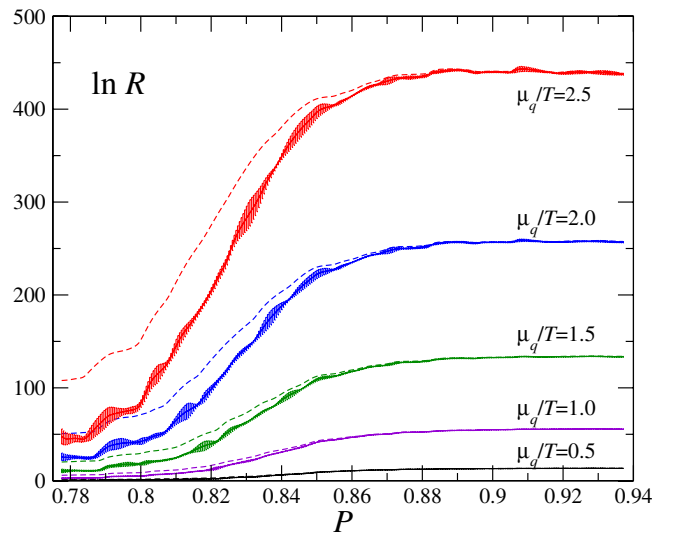


FIG. 5 (color online). The reweighting factor  $R(P, \mu_q)$  for  $\mu_q/T = 0.5-2.5$  obtained by the Taylor expansion up to  $O(\mu_q^6)$ . The dashed lines are the cases when the effect of the complex phase is omitted,  $\tilde{R}(P, \mu_q)$ .

Because  $R(P, \mu_q)$  is independent of  $\beta$ , we mix all data obtained at different  $\beta$ . This mixture can be justified by extending Eq. (18) for multi- $\beta$ , e.g.  $R(P', \mu_q) = [N_1 \langle \delta(P' - P)F \rangle_{\beta_1} + N_2 \langle \delta(P' - P)F \rangle_{\beta_2}] / [N_1 \langle \delta(P' - P) \rangle_{\beta_1} + N_2 \langle \delta(P' - P) \rangle_{\beta_2}]$  for the data at  $\beta_1$  and  $\beta_2$  with the number of configurations  $N_1$  and  $N_2$ . The results for  $\ln R(P, \mu_q)$  are shown by solid lines in Fig. 5 for  $\mu_q/T = 0.5, 1.0, 1.5, 2.0$  and  $2.5$ . We find a rapid change in  $\ln R$  around  $P \sim 0.83$ , and the variation becomes larger as  $\mu_q/T$  increases.

The dashed lines in Fig. 5 are the results that we obtained when the effect of the complex phase, i.e.  $\exp[-1/(4a_2)]$ , is omitted. We define this quantity as

$$\bar{R}(P', \mu_q) \equiv \frac{\langle |F(\mu_q)| \delta(P' - P) \rangle_{(T, \mu_q=0)}}{\langle \delta(P' - P) \rangle_{(T, \mu_q=0)}}. \quad (41)$$

We discuss in Sec. III G that these dashed lines correspond to the reweighting factor with nonzero isospin chemical potential  $\mu_I$  and zero quark chemical potential  $\mu_q$ , i.e.  $\bar{R}(P, \mu_q) = R(P, \mu_I)$ . The variation of  $\ln R$  in terms of  $P$  becomes milder when the effect of the complex phase is omitted.

The effective potential  $V(P, \beta, \mu_q)$  is obtained from Eq. (20) substituting the data in Figs. 3 and 5. To study the existence of a second order phase transition, the curvature of the potential is important. The minimum of the potential can be changed by shifting  $\beta$  but the curvature can be controlled only by  $\ln R(P, \mu_q)$ . The result of the curvature at  $\mu_q = 0$ ,  $-d^2(\ln w)/dP^2$ , as a function of  $P$  is shown in Fig. 4. Because  $-d^2(\ln w)/dP^2$  is positive, a region where  $d^2(\ln R)/dP^2 > 0$  is necessary for the existence of a critical point. The curvature of  $\ln R$  is positive for  $P \leq 0.83$ .

In order to analyze the sign of  $d^2V/dP^2(P, \mu_q)$ , we fitted the data around  $P$  by a quadratic function,  $\ln R(P', \mu_q) = x_0 + x_1(P' - P) + x_2(P' - P)^2$ , where  $x_0$ ,  $x_1$ , and  $x_2$  are the fit parameters, and calculate the first and second derivatives of  $\ln R(P, \mu_q)$  at each  $P$ . The result of the slope,  $d(\ln R)/dP(P, \mu_q) = x_1$ , is shown in Fig. 6 for each  $\mu_q/T$ . We adopt the result obtained by fitting in the range between  $P - 0.015$  and  $P + 0.015$  for each  $P$  as the final result. In the region around  $P \sim 0.83$ ,  $d(\ln R)/dP$  becomes larger as  $\mu_q/T$  increases and  $\ln R(P, \mu_q)$  changes sharply in this region. The result of the curvature,  $d^2(\ln R)/dP^2(P, \mu_q) = 2x_2$ , is plotted as solid line in Fig. 7. The magnitude of the curvature of  $\ln R$  also becomes larger as  $\mu_q/T$  increases. The dashed line in Fig. 7 is the data of  $-d^2(\ln w)/dP^2(P)$  in Fig. 4. This figure indicates that the maximum value of  $d^2(\ln R)/dP^2(P, \mu_q)$  at  $P = 0.80$  becomes larger than  $-d^2(\ln w)/dP^2$  for  $\mu_q/T \geq 2.5$ . This suggests that the curvature of the effective potential,  $d^2V/dP^2 = -d^2(\ln w)/dP^2 - d^2(\ln R)/dP^2$ , vanishes at

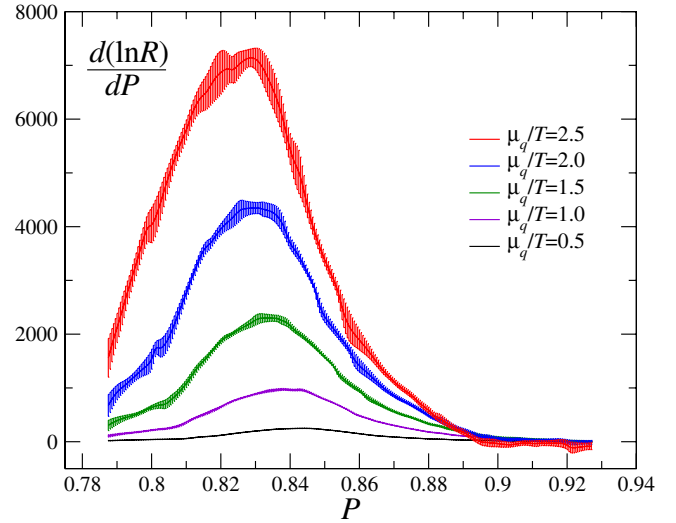


FIG. 6 (color online). The slope of  $\ln R(P, \mu_q)$  as functions of the plaquette.

$\mu_q/T \sim 2.5$  and a region of  $P$  where the curvature is negative appears for large  $\mu_q/T$ .

Next, we estimate the value of  $\beta$  which gives the potential minimum at  $P = 0.8$  for  $\mu_q/T = 2.5$  by solving the equation:

$$\frac{dV}{dP}(P, \beta, \mu_q) = -\frac{d(\ln R)}{dP}(P, \mu_q) - \frac{d(\ln w)}{dP}(P, \beta_0) - 6(\beta - \beta_0)N_{\text{site}} = 0. \quad (42)$$

This equation can be solved without changing  $\mu_q/T$  and tells us the location of the critical point in the  $(\beta, \mu_q/T)$  plane. Since a simulation with  $\beta \approx 3.56$  gives  $d(\ln w)/dP = 0$  at  $P \approx 0.8$ , we adopt  $\beta_0 = 3.56$ .

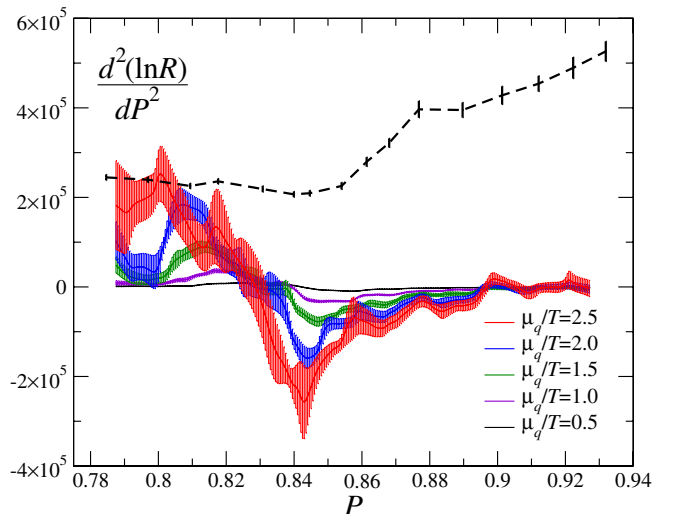


FIG. 7 (color online). The curvature of  $\ln R(P, \mu_q)$  as functions of the plaquette. The dashed line is the curvature of  $-\ln w$ .

Substituting  $d(\ln R)/dP \approx 4000$  at  $(P, \mu_q/T) = (0.8, 2.5)$  in Fig. 6 and  $N_{\text{site}} = 16^3 \times 4$ , we obtain  $\beta \approx 3.52$ . This  $\beta$  corresponds to  $T/T_c = 0.76$ , where  $T_c$  is the pseudocritical temperature at  $\mu_q = 0$ . Therefore, it is found that the potential is flat up to second order in  $P$  around  $P = 0.80$  with  $(T/T_c, \mu_q/T) \approx (0.76, 2.5)$ , suggesting the existence of a critical point around this value.

Further studies are, of course, needed for the precise determination of the critical point in the  $(T, \mu_q)$  plane, increasing the number of terms in the Taylor expansion of  $\ln \det M$  and decreasing the quark mass in the simulation. The quark mass is still heavier than the physical quark mass. However, the arguments given above indicate the existence of a first order phase transition line at large  $\mu_q/T$  because the magnitude of the curvature of  $R(P, \mu_q)$  increases monotonically and eventually the curvature of the potential becomes negative at large  $\mu_q/T$ , corresponding to a double-well potential of a first order phase transition.

### F. Application range of this analysis

Next, we discuss the reliability of our analysis in view of the truncation of the Taylor expansion used here. Because the dominant contribution in  $\ln R$  is given by the reweighting factor without the phase effect,  $\ln \bar{R}$ , we consider the radius of convergence for  $\ln \bar{R}$ . The expansion is defined by

$$\ln \bar{R}(P, \mu_q) = \sum_{n=1}^{\infty} \bar{r}_n(P) \left( \frac{\mu_q}{T} \right)^n, \quad (43)$$

$$\begin{aligned} \bar{r}_2 &= \langle d_2 \rangle_P, & \bar{r}_4 &= \langle d_4 \rangle_P + \frac{1}{2}(\langle d_2^2 \rangle_P - \langle d_2 \rangle_P^2), \\ \bar{r}_6 &= \langle d_6 \rangle_P + \langle d_2 d_4 \rangle_P - \langle d_2 \rangle_P \langle d_4 \rangle_P + \frac{1}{6}(\langle d_2^3 \rangle_P \\ &\quad - 3\langle d_2 \rangle_P \langle d_2^2 \rangle_P + 2\langle d_2 \rangle_P^3), \end{aligned} \quad (44)$$

where  $d_n = (N_f/n!) \partial^n (\ln \det M) / \partial (\mu_q/T)^n$ ,  $\langle \dots \rangle_{P'} = \langle \dots \delta(P' - P) \rangle / \langle \delta(P' - P) \rangle$ , and the odd terms are zero. The radius of convergence is obtained by analyzing the asymptotic behavior of  $\rho_n = \sqrt{|\bar{r}_n / \bar{r}_{n+2}|}$  for  $n = 2, 4, 6, \dots, \infty$ .

In this analysis, we calculated  $\ln \det M$  using the data of  $d_n$  up to  $O(\mu_q^6)$ . This approximation does not affect the calculations of  $\bar{r}_2$ ,  $\bar{r}_4$ , and  $\bar{r}_6$ , but there is a missing term, i.e.  $\langle d_8 \rangle_P$ , in the calculation of  $\bar{r}_8$ . If the 8th order term of  $\ln R$  is larger than the 6th order term, the effect of the truncation may be sizeable. Because  $|\bar{r}_6(\mu_q/T)^6| > |\bar{r}_8(\mu_q/T)^8|$  for  $\mu_q/T < \rho_6$ , the application range for our current analysis should be  $\mu_q/T \leq \rho_6$ . We calculate  $\rho_2$  and  $\rho_4$ . These results are shown in Fig. 8. The dashed line is  $\rho_2$  in the free gas limit, and  $\rho_4$  is infinity in the free gas limit. The results of  $\bar{r}_2$  and  $\bar{r}_4$  are positive for all  $P$  we investigated, but  $\bar{r}_6$  changes its sign at  $P = 0.84$ .  $\bar{r}_6$  is negative for  $P \geq 0.84$ . We find that  $\rho_4$  (square) is larger than  $\rho_2$  (circle), and the values of  $\rho_2$  and  $\rho_4$  are larger than the hadron resonance gas model values,  $\rho_2 \approx 1.15$  and

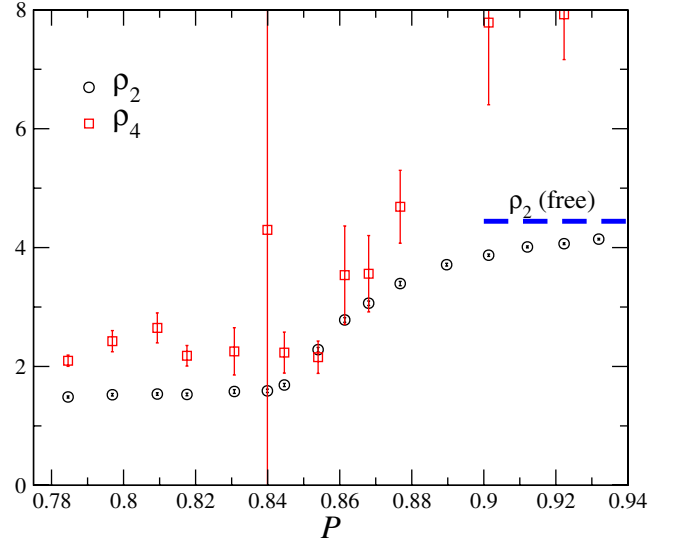


FIG. 8 (color online). The radius of convergence,  $\rho_2$ ,  $\rho_4$ , for the Taylor expansion of  $\bar{R}(P, \mu_q)$ .

$\rho_4 \approx 1.83$ . For our analysis, where we omitted the calculation of  $d_n$  higher than the 6th order in  $\ln R$ , the application range given by  $\rho_6$  would be larger than the hadron resonance gas model prediction,  $\rho_6 \approx 2.49$ , and the parameter range we investigated thus seems to be within the application range.

We moreover estimate the effect from higher order terms in the Taylor expansion by changing the number of terms in the Taylor expansion. Figure 9 shows the difference between the results up to  $O(\mu_q^4)$  and  $O(\mu_q^6)$  for  $\mu_q/T = 0.5, 1.0, 1.5$ , and  $2.5$ . The dashed lines are the same as the solid lines in Fig. 5 and the solid lines are the results obtained

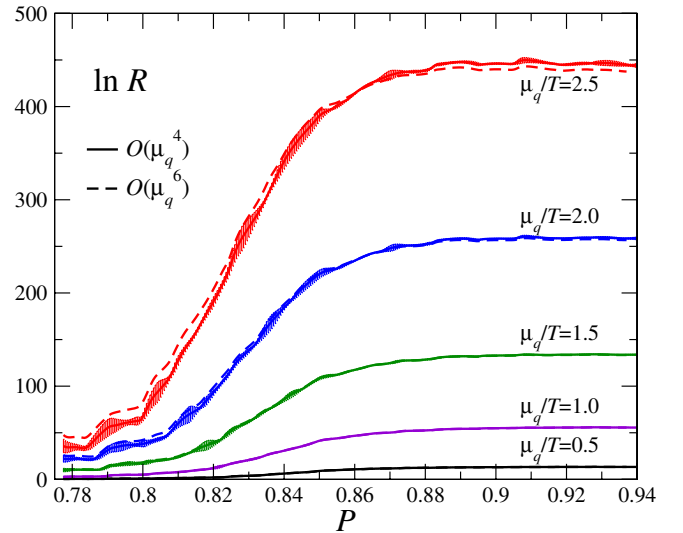


FIG. 9 (color online). The reweighting factor  $R(P, \mu_q)$  computed by the Taylor expansion up to  $O(\mu_q^4)$  (solid lines) and  $O(\mu_q^6)$  (dashed lines).

when the highest order term and the next highest order term,  $d^6(\ln M)/d(\mu_q/T)^6$  and  $d^5(\ln M)/d(\mu_q/T)^5$ , are omitted in Eq. (21). It is found from this figure that the difference becomes visible at  $\mu_q/T \sim 2.5$ , but the truncation error of the Taylor expansion does not affect the qualitative argument of the effective potential at finite density in the range we have discussed. For more quantitative investigation of the critical point in the  $(T, \mu_q)$  plane, more accurate calculations including higher order terms in the Taylor expansion of  $\mu_q$  may be important.

### G. QCD with an isospin chemical potential

Finally, it is worth discussing the difference between QCD with a quark (baryon) chemical potential and an isospin chemical potential. The isospin chemical potential is defined by  $\mu_I = (\mu_u - \mu_d)/2$ , where  $\mu_u$  and  $\mu_d$  are the chemical potential for  $u$  and  $d$  quarks, respectively. For the case with nonzero isospin and zero quark chemical potentials,  $\mu_q = (\mu_u + \mu_d)/2 = 0$ , i.e.  $\mu_u = -\mu_d = \mu_I$ , the quark determinant is real and positive because

$$\begin{aligned} \det M(\mu_u) \det M(\mu_d) &= \det M(\mu_I) \det M(-\mu_I) \\ &= \det M(\mu_I) (\det M(\mu_I))^* \\ &= |\det M(\mu_I)|^2 \end{aligned} \quad (45)$$

where we used an identity at finite  $\mu_q$ ,  $\gamma_5 M(\mu_q) \gamma_5 = M(-\mu_q)^\dagger$ . Therefore, Monte Carlo simulations are possible for this case [30], and the simulations with the isospin chemical potential have been performed in Refs. [18,19,28,31,32]. It may be important toward the understanding of QCD at finite density to consider the difference between the phase diagram with nonzero baryon chemical and that with nonzero isospin chemical potential.

The reweighting factor  $\bar{R}$ , i.e. the dashed line in Fig. 5, corresponds to the reweighting factor of the isospin chemical potential  $R(P, \mu_I)$  for each  $\mu_I/T$  because the quark determinant is  $|\det M(\mu_q)|^2$ . It is found from Fig. 5 that the slope and the curvature of  $\ln R$  around  $P \sim 0.82$  for the isospin chemical potential are smaller than those for the quark chemical potential. This means that the value of  $\mu_I/T$  where the second order phase transition appears by canceling the curvatures of  $\ln w(P, \beta)$  and  $\ln R(P, \mu_I)$  is larger than the critical point of  $\mu_q/T$ . It is suggested in Ref. [19] that there is no first order phase transition region in the low density regime of QCD with nonzero  $\mu_I/T$ . Although more quantitative estimations of the reweighting factor are needed to confirm the existence of the first order transition line, our argument may be related to their result.

Furthermore, in the case of the approximation up to  $O(\mu_q^2)$ ,  $R(P, \mu_q)$  and  $R(P, \mu_I)$  have a close relation to the quark number susceptibility  $\chi_q$  and isospin susceptibility  $\chi_I$  at  $\mu_{q,I} = 0$ . Using the Eqs. (28), (29), and (33),

$$\begin{aligned} \ln R(P, \mu_q) &\approx \ln \left\langle \exp \left[ \frac{1}{2} N_f \operatorname{Re} \frac{\partial^2 (\ln \det M)}{\partial (\mu_q/T)^2} \left( \frac{\mu_q}{T} \right)^2 \right] \right\rangle_P \\ &\quad - \frac{1}{2} \left\langle \left( N_f \operatorname{Im} \frac{\partial (\ln \det M)}{\partial (\mu_q/T)} \frac{\mu_q}{T} \right)^2 \right\rangle_P \\ &\approx \frac{1}{2} \left[ \left\langle N_f \frac{\partial^2 (\ln \det M)}{\partial (\mu_q/T)^2} + \left( N_f \frac{\partial (\ln \det M)}{\partial (\mu_q/T)} \right)^2 \right\rangle_P \right] \\ &\quad \times \left( \frac{\mu_q}{T} \right)^2 \end{aligned} \quad (46)$$

in this approximation, and when the effect from  $\theta$  is omitted, we find

$$\ln R(P, \mu_I) = \ln \bar{R}(P, \mu_q) \approx \frac{1}{2} \left\langle N_f \frac{\partial^2 (\ln \det M)}{\partial (\mu_q/T)^2} \right\rangle_P \left( \frac{\mu_q}{T} \right)^2, \quad (47)$$

where  $\langle \dots \rangle_{P'} = \langle \dots \delta(P' - P) \rangle / \langle \delta(P' - P) \rangle$ . These are related to  $\chi_q/T^2$  and  $\chi_I/T^2$  as functions of  $\beta$  (temperature) by the following equations:

$$\begin{aligned} \frac{\chi_q}{T^2}(T, \mu_{q,I} = 0) &= \frac{N_f^3}{N_s^3} \frac{1}{Z} \int \left\langle N_f \frac{\partial^2 (\ln \det M)}{\partial (\mu_q/T)^2} \right. \\ &\quad \left. + \left( N_f \frac{\partial (\ln \det M)}{\partial (\mu_q/T)} \right)^2 \right\rangle_P w(P, \beta) dP, \end{aligned} \quad (48)$$

$$\frac{\chi_I}{T^2}(T, \mu_{q,I} = 0) = \frac{N_f^3}{N_s^3} \frac{1}{Z} \int \left\langle N_f \frac{\partial^2 (\ln \det M)}{\partial (\mu_q/T)^2} \right\rangle_P w(P, \beta) dP. \quad (49)$$

From these equations, the similarity between the figures for  $R(P, \mu_{q,I})$  and those of the quark number and isospin susceptibilities can be easily understood in the regime where the Taylor expansion is valid. As shown in Fig. 3,  $w(P, \beta)$  is a Gaussian function having a sharp peak. Therefore, Fig. 5 is quite similar to Fig. 1 in Ref. [7] if we replace the horizontal axis  $P$  by  $T/T_c(\beta)$ . As we have discussed, the positive curvature in the  $P$  dependence of  $\ln R(P, \mu_q)$  is required for the appearance of the critical endpoint. It is found that the positive curvature is related closely to the rapid increase of the quark number susceptibility near the pseudocritical temperature at  $\mu_q = 0$ .

Here, it should be noted that  $\chi_I/T^2$  is always larger than  $\chi_q/T^2$  at  $\mu_q = 0$  because  $\partial (\ln \det M) / \partial (\mu_q/T)$  is purely imaginary, and thus  $(\partial (\ln \det M) / \partial (\mu_q/T))^2$  is negative. Moreover, both susceptibilities approach the same value in the high temperature limit. Hence, the variation of  $\chi_I/T^2$  around the transition point would be milder than that of  $\chi_q/T^2$ , corresponding to the behavior of  $R(P, \mu_q)$  and  $R(P, \mu_I)$ . This may explain the difference between the phase diagrams with finite  $\mu_q$  and finite  $\mu_I$ . Furthermore, in the framework of the hadron resonance

gas model at low temperature, the isospin susceptibility corresponds to fluctuations of pions, and the pion mass is more sensitive to the quark mass than baryon masses. Therefore, when the quark mass is decreased, the pion mass becomes smaller and the fluctuation becomes larger at low temperature. This suggests the change of  $\chi_I/T^2$  around  $T_c$  may be milder at small quark mass, i.e. the difference between  $\ln R(P, \mu_q)$  and  $\ln R(P, \mu_I)$  becomes large at small quark mass.

For more precise arguments on the phase structure, more accurate evaluations of  $R(P, \mu_q)$  and  $R(P, \mu_I)$  are required increasing the number of terms in the Taylor expansion of  $\ln \det M$ . However, the qualitative property that the critical value of  $\mu_q/T$  in the  $(T, \mu_q)$  plane is smaller than the critical  $\mu_I/T$  in the  $(T, \mu_I)$  plane can be understood by the well-known properties of the quark (baryon) number and isospin susceptibilities combined with the argument of the effective potential.

#### IV. CONCLUSIONS

We have discussed the phase structure of lattice QCD at nonzero density. The probability distribution as a function of the plaquette was estimated at nonzero temperature and chemical potential using the data obtained with two-flavors of p4-improved staggered quarks in Ref. [7]. In this analysis, we have adopted two approximations. One is that we estimate  $\ln \det M$  from the data of a Taylor expansion up to  $O(\mu_q^6)$ . Terms of higher order than  $\mu_q^6$  are omitted. We have estimated the range where this approximation is valid and studied in the reliability range. The second approximation is an assumption on the probability distribution for

the complex phase. We have assumed the distribution function to be a Gaussian function. This assumption will be valid for sufficiently large volume and we have checked that the distribution is well approximated by a Gaussian function for the data used in this analysis.

In spite of the use of these approximations, it is found that the shape of the effective potential which is of Gaussian type at  $\mu_q = 0$  changes to a double-well type at large  $\mu_q/T$ . This property is related closely to a well-known behavior of the quark number susceptibility at  $\mu_q = 0$ , i.e. the rapid increase near the phase transition point. For the quantitative estimation of the endpoint of the first order phase transition, further investigation is needed. However, this argument strongly suggests the existence of the first order phase transition line in the  $(T, \mu_q)$  plane.

We also discussed the difference between QCD with a quark chemical potential and QCD with an isospin chemical potential, and found that the critical value of the quark chemical potential seems to be smaller than that of the isospin chemical potential.

#### ACKNOWLEDGMENTS

I would like to thank F. Karsch, K. Kanaya, T. Hatsuda, S. Aoki, T. Izubuchi, and K. Fukushima for discussions and comments. This work has been authored under Contract No. DE-AC02-98CH10886 with the U.S. Department of Energy. I also wish to thank the Sumitomo Foundation for their financial assistance (No. 050408) and the Yukawa Institute for Theoretical Physics at Kyoto University for discussions during the YITP workshops YITP-W-06-07 and YKIS2006.

- 
- [1] Z. Fodor and S. Katz, Phys. Lett. B **534**, 87 (2002).
  - [2] Z. Fodor and S. Katz, J. High Energy Phys. 03 (2002) 014; 04 (2004) 050.
  - [3] C.R. Allton, S. Ejiri, S.J. Hands, O. Kaczmarek, F. Karsch, E. Laermann, Ch. Schmidt, and L. Scorzato, Phys. Rev. D **66**, 074507 (2002).
  - [4] P. de Forcrand and O. Philipsen, Nucl. Phys. **B642**, 290 (2002).
  - [5] M. D'Elia and M.-P. Lombardo, Phys. Rev. D **67**, 014505 (2003).
  - [6] C.R. Allton, S. Ejiri, S.J. Hands, O. Kaczmarek, F. Karsch, E. Laermann, and C. Schmidt, Phys. Rev. D **68**, 014507 (2003).
  - [7] C.R. Allton, M. Döring, S. Ejiri, S.J. Hands, O. Kaczmarek, F. Karsch, E. Laermann, and K. Redlich, Phys. Rev. D **71**, 054508 (2005).
  - [8] S. Ejiri, F. Karsch, E. Laermann, and C. Schmidt, Phys. Rev. D **73**, 054506 (2006).
  - [9] C. Bernard *et al.*, Proc. Sci., LAT2006 (2006) 139 [arXiv:hep-lat/0610017].
  - [10] M. Asakawa and K. Yazaki, Nucl. Phys. **A504**, 668 (1989).
  - [11] A. Barducci, R. Casalbuoni, S. De Curtis, R. Gatto, and G. Pettini, Phys. Lett. B **231**, 463 (1989); Phys. Rev. D **41**, 1610 (1990); A. Barducci, R. Casalbuoni, G. Pettini, and R. Gatto, Phys. Rev. D **49**, 426 (1994).
  - [12] M. Stephanov, K. Rajagopal, and E. Shuryak, Phys. Rev. Lett. **81**, 4816 (1998).
  - [13] S. Ejiri, Phys. Rev. D **73**, 054502 (2006).
  - [14] R. V. Gavai and S. Gupta, Phys. Rev. D **71**, 114014 (2005).
  - [15] Ch. Schmidt, C.R. Allton, S. Ejiri, S.J. Hands, O. Kaczmarek, F. Karsch, and E. Laermann, Nucl. Phys. B, Proc. Suppl. **119**, 517 (2003); F. Karsch, C.R. Allton, S. Ejiri, S.J. Hands, O. Kaczmarek, E. Laermann, and Ch. Schmidt, Nucl. Phys. B, Proc. Suppl. **129**, 614 (2004); S. Ejiri, C.R. Allton, S.J. Hands, O. Kaczmarek, F. Karsch, E. Laermann, and Ch. Schmidt, Prog. Theor. Phys. Suppl. **153**, 118 (2004).
  - [16] P. de Forcrand and O. Philipsen, Nucl. Phys. **B673**, 170 (2003); J. High Energy Phys. 01 (2007) 077.

- [17] M. D'Elia and M.-P. Lombardo, *Phys. Rev. D* **70**, 074509 (2004).
- [18] J. B. Kogut and D. K. Sinclair, arXiv:hep-lat/0509095.
- [19] J. B. Kogut and D. K. Sinclair, *Proc. Sci., LAT2006* (2006) 147 [arXiv:hep-lat/0609041].
- [20] Z. Fodor, S. Katz, and C. Schmidt, *J. High Energy Phys.* **03** (2007) 121.
- [21] A. M. Ferrenberg and R. H. Swendsen, *Phys. Rev. Lett.* **61**, 2635 (1988); *Phys. Rev. Lett.* **63**, 1195 (1989).
- [22] I. M. Barbour, S. E. Morrison, E. G. Klepfish, J. B. Kogut, and M.-P. Lombardo, *Phys. Rev. D* **56**, 7063 (1997).
- [23] K. Splittorff, *Proc. Sci. LAT2006* (2006) 023; K. Splittorff and J. J. M. Verbaarschot, *Phys. Rev. Lett.* **98**, 031601 (2007).
- [24] S. Ejiri, *Phys. Rev. D* **69**, 094506 (2004).
- [25] F. Karsch, E. Laermann, and C. Schmidt, *Phys. Lett. B* **520**, 41 (2001).
- [26] A. Gocksch, *Phys. Rev. Lett.* **61**, 2054 (1988).
- [27] K. N. Anagnostopoulos and J. Nishimura, *Phys. Rev. D* **66**, 106008 (2002); J. Ambjorn, K. N. Anagnostopoulos, J. Nishimura, and J. J. M. Verbaarschot, *J. High Energy Phys.* **10** (2002) 062.
- [28] T. Takaishi, *Mod. Phys. Lett. A* **19**, 909 (2004).
- [29] F. Karsch, K. Redlich, and A. Tawfik, *Eur. Phys. J. C* **29**, 549 (2003); *Phys. Lett. B* **571**, 67 (2003).
- [30] D. T. Son and M. A. Stephanov, *Phys. Rev. Lett.* **86**, 592 (2001).
- [31] J. B. Kogut and D. K. Sinclair, *Phys. Rev. D* **66**, 034505 (2002).
- [32] A. Nakamura and T. Takaishi, *Nucl. Phys. B, Proc. Suppl.* **129**, 629 (2004).